Electrochemical Oxidation of Single Wall Carbon Nanotube Bundles in Sulfuric Acid

G. U. Sumanasekera,[†] J. L. Allen,[†,‡] S. L. Fang,[†,‡] A. L. Loper,[†] A. M. Rao,[‡] and P. C. Eklund*[,†,‡]

Department of Physics and Astronomy and Center for Applied Energy Research, University of Kentucky, Lexington, Kentucky 40506

Received: November 9, 1998

Electrochemical doping of bisulfate ions into single wall carbon nanotube (SWNT) bundles has been studied using coulometry, cyclic voltammetry, mass-uptake measurements, and Raman scattering experiments. A spontaneous charge-transfer reaction is observed prior to the application of an electrochemical driving force, in sharp contrast to previous observations in the graphite−H_2SO_4 system. A mass increase of the SWNT sample and a concomitant upshift of the Raman-active tangential mode frequency indicate oxidation (i.e., removal of electrons) of the SWNT bundles. In fact, using Raman scattering, we were able to separate the spontaneous and electrochemical contributions to the overall charge transfer, resulting in the value of an upshift of 320 cm^{-1} per hole, per C-atom introduced into the carbon π-band by the bisulfate (HSO_4^-) dopant. This value may prove to be a universal measure of charge transfer in acceptor-type SWNT compounds. At a critical electrochemical doping, the SWNT bundles are driven into an "overoxidation" regime, where they are irreversibly oxidized with the formation of C−O covalent bonds, analogous to electrochemical formation of graphite oxides.

Introduction

Graphite's lamellar structure with weak van der Waals interlayer bonding between the graphene sheets, and its amphoteric nature, have allowed the synthesis of a large number of donor and acceptor graphite intercalation compounds (GICs) in which sheets of intercalated atoms or molecules are inserted between the host graphene planes.[1] Of particular interest to the present work here on single wall carbon nanotubes (SWNTs), graphite−bisulfate intercalation compounds $C_p^+HSO_4^-(xH_2SO_4)$ have been prepared by both chemical[2] and electrochemical oxidation of graphite in sulfuric acid.[3,4] The electrochemical oxidation of graphite (i.e., removal of electrons) in sulfuric acid, first reported by Rüdorff,[3] has been shown to provide an exact determination of charge transfer ($f = 1/p$) between the host carbon and guest intercalate layers through coulometry. Thus these compounds provided a convenient means to study the effect of charge transfer on the physical properties of acceptor GICs. A large number of studies devoted to graphite-bisulfate intercalation compounds then followed.[5−27]

A single wall carbon nanotube (SWNT) can be envisioned as a long, rolled up graphene sheet with a seamless joint.[28] The SWNT exhibits a well-defined, periodic structure defined by the "roll up" vector $\mathbf{C}(n,m) = n\mathbf{a} + m\mathbf{b}$, where **a** and **b** are primitive translation vectors of the graphene sheet, and n and m are integers. The symmetry, unit cell dimension, and tube diameter are uniquely determined by the integers (n, m) and the carbon interatomic distance. SWNTs prepared by pulsed laser vaporization (PLV)[30] and the arc discharge (AD)[29] methods have been shown by transmission electron microscopy (TEM) to self-organize into bundles containing tens to hundreds of tubes held in a triangular "rope" lattice by the van der Waals force.[30] Thus, by analogy to GICs, it was expected that bundles of SWNTs could be oxidatively (reductively) intercalated, where the guest anions (cations) occupy sites in the interstitial channels in the rope lattice. Evidence for the existence of such compounds has been demonstrated recently for alkali metal and halogen vapor-phase-doped SWNTs.[31−34] Doping provides an attractive means of controlling the electronic properties of SWNTs. Here, we present a study of the electrochemical anodic oxidation of SWNTs in sulfuric acid. In situ Raman scattering and mass uptake were used to study the guest−host charge-transfer chemistry. Interesting comparisons can be made for the anodic oxidation of graphite and SWNT hosts in sulfuric acid, and they will be discussed below.

Experimental Section

ACS reagent grade sulfuric acid (H_2SO_4 95%, Fisher Scientific, as received) was used and diluted with distilled water as needed. Pressed pellet mats of SWNT bundles containing coproduced carbon nanoparticles synthesized by the electric arc discharge (AD) and pulsed laser vaporization (PLV) process were studied, giving very similar electrochemical results. The SWNTs obtained from both these processes exhibited a narrow diameter distribution with a most probable diameter in the range 1.3−1.4 nm. The diameter of a (10, 10) armchair nanotube is 1.37 nm. In a separate experiment, the coproduced carbon nanoparticles were found not to be electrochemically active.

Electrochemical reactions were carried out in a closed quartz cell with the standard three-electrode configuration. The quartz cell allowed in situ Raman spectroscopy of the SWNTs during anodic oxidation, and this cell has been described previously.[23] Typically, a mat of SWNTs ($4 \times 4 \times 0.1$ mm^3) was pressed onto a platinum (Pt) plate and used as the "working" electrode. A Pt wire served as the "counter" electrode and the cell potential was measured between a "reference" electrode (saturated calomel electrode, or SCE) and the working electrode.

* To whom correspondence should be addressed.
[†] Department of Physics and Astronomy.
[‡] Center for Applied Energy Research.

10.1021/jp984362t CCC: $18.00
Published on Web 04/30/1999

A model 273 EG&G Princeton Applied Research potentiostat/galvanostat provided electrochemical control during the measurements. Controlled current (galvanostatic) reactions were performed by allowing a constant current to flow between the working and counter electrodes. The potential between the working and SCE electrodes was measured as a function of time t or charge $Q = I_0 t$, where I_0 = constant current. When the electrons passed through the external circuit from the SWNT electrode to the Pt counter electrode, anodic oxidation of the SWNTs was confirmed by in situ Raman scattering.

Controlled potential (potentiostatic) reactions were also studied. In this case, the potential difference between the working and counter electrodes was stepped at a rate of ca. 0.1 mV/s from ~0 to ~1.5 V and back again in a cyclic fashion. The resulting cyclic voltammograms, indicating the charge passed during each voltage step, were also recorded vs the cell potential.

In situ Raman spectra of the intercalated SWNT rope lattice were recorded in the backscattering configuration during both the cyclic voltammetry and the constant current reactions. Radiation from an argon ion laser (514.5 nm) was focused with a cylindrical lens onto the sample; the power density was ~2 W cm^{-2}. The spectra were collected with a single-grating instrument (Jobin Yvon HR460; ISA, Inc.) equipped with a charge-coupled array detector (CCD) and an external holographic notch filter (Kaiser Optical Systems, Inc.).

In independent experiments, the mass uptake of the SWNT electrode was also obtained during anodic oxidation. This was accomplished by hanging the SWNT working electrode by a fine Pt wire from the arm of an analytical balance (sensitivity 10 μg) and suspending the sample in a beaker of H_2SO_4, which also contained the Pt counter electrode and the SCE reference electrode.

Results and Discussion

Graphite−bisulfate intercalation compounds have been known for almost 160 years since Schafhäutl observed dilation of graphite during exposure to boiling sulfuric acid.[5] In 1954, Rüdorff and Hoffman first reported the electrochemical preparation from a natural single crystal of graphite.[3,4] At the same time, they discovered the "staging" phenomenon whereby a periodic stacking of carbon and bisulfate layers were formed, e.g., a "stage 4" material has the layer stacking sequence ...IC′CCC′IC′CCC′I..., where C′ is a "bounding" carbon layer, C is an "interior" carbon layer, and I is a bisulfate layer.[3,4] That is, the stage number (n) refers to the number of carbon layers separating successive intercalate layers. They established an approximate stoichiometry of the first stage (...C′IC′I...) compound as $C_{24}^{+}(HSO_4^{-})\cdot 2H_2SO_4$, where the amount of charge transferred between the graphite host and new (guest) $HSO_4^{-}\cdot xH_2SO_4$ layers was calculated from the constant external current (I_0) passed during a specific time Δt; the amount of neutral H_2SO_4 molecules coexisting in the intercalate layers with the HSO_4^{-} (bisulfate) ions was determined by mass uptake (gravimetry). Later electrochemical studies[14] established that a *range* of stage 1 and stage 2 graphite−H_2SO_4 compounds ($C_p^{+}HSO_4^{-}\cdot xH_2SO_4$) could be prepared: $56 < p < 48$ (stage 2) and $28 < p < 24$ (stage 1). This was proposed to be accomplished by an "overcharging" mechanism in which the cell potential drives the internal conversion of neutral sulfuric acid molecules to bisulfate anions, i.e., $H_2SO_4 + e^{-} \rightarrow HSO_4^{-} + {}^1/_2H_2$ in the intercalate layers.[14] For charge neutrality in the GIC, additional charge transfer between the carbon and the intercalate layers was then necessary to accommodate the additional bisulfate ion formation during "overcharging". Above a cell potential of 1 V, "overcharging" in a stage 1 GIC was found to stop, and an "overoxidation" regime commences, in which the presence of H_2O in the sulfuric acid allows the electrochemical formation of C−O bonds and the graphitic network in the graphene sheet is irreversibly altered. Eventually, a "graphite oxide" can be formed electrochemically, which is a highly disordered compound containing C, H, and O.[36]

The total charge transfer between carbon and intercalate layers in the compound $C_p^{+}HSO_4^{-}\cdot xH_2SO_4$ can be represented by $f = 1/p$, where f is the number of mobile holes per C-atom in the carbon π-band. f is calculated according to

$$f = 1/p = Q/m_0(M/N_A e) \qquad (1)$$

where Q is the electrochemical charge passed in the circuit, m_0 is the mass of the SWNTs, M is the molecular weight of carbon, N_A is Avogadro's number, and e is the charge of the electron. To correct the sample mass m to the SWNT mass m_0, we use (1) the estimated yield of ~70% of the sample carbon in SWNTs[30] and (2) the assumption that the same weight percent of the catalyst in the electrode (target) ends up in the as-prepared SWNT mat.

For electrochemical insertion of H_2SO_4 and HSO_4^{-} into graphite we have[33]

$$(1)\ e^{-} + H_2SO_4 \rightarrow {}^1/_2H_2 + HSO_4^{-} \qquad \text{(cathode)}$$

$$(2)\ C_p^{+}HSO_4^{-} + vH_2SO_4 \rightarrow C_p^{+}HSO_4^{-}\cdot vH_2SO_4 + e^{-} \qquad \text{(anode)}$$

During "overcharging" we have

$$(3)\ C_p^{+}HSO_4^{-}\cdot vH_2SO_4 \rightarrow C_p^{(1+\delta)+}(HSO_4^{-})_{(1+\delta)}\cdot (v-\delta)H_2SO_4 + \delta e^{-} + \delta H^{+} \qquad \text{(anode)}$$

$$(4)\ \delta H^{+} + \delta e^{-} \rightarrow \delta/2H_2 \qquad \text{(cathode)}$$

Raman scattering spectroscopy applied to various all-carbon solids have been reviewed recently.[37−43] In both fullerenes and graphite intercalation compounds, the high-frequency, Raman-active modes have been shown to be a sensitive probe of charge transfer between the carbon host and intercalated guest ions introduced into the structure. Of considerable importance to the work presented here, are detailed studies of the Raman-active modes in graphite-H_2SO_4 GICs prepared electrochemically.[23] In that work, it was found that the high-frequency carbon mode associated with the intralayer displacement of carbon atoms in the bonding (C′) carbon layers upshifts linearly in frequency with charge-transfer f. This upshift in mode frequency was identified with a charge-transfer induced contraction of the C−C bonds.[23] During "overcharging" in stage 1 and stage 2 graphite-H_2SO_4, a continuous shift with electrochemical charge Q of the C′-layer mode frequency ω was reported. Values for this shift of $d\omega/df = 460$ cm^{-1}, $d\omega/df = 1200$ cm^{-1} were reported for stage 1 and stage 2, respectively.

More recently, it has been show that Raman scattering is also an effective probe of single wall carbon nanotubes.[31,33] The high-frequency tangential displacement SWNT modes near ~1593 cm^{-1}, which are related to the C′ intralayer modes in a GIC, were found sensitive to the charge exchanged between the nanotubes and guest ions that have intercalated into the interstitial channels in the tube bundles.[31]

Based on the previous in situ Raman results reported for graphite-H_2SO_4 GICs, we were quite surprised to observe the rapid *spontaneous* shift of the SWNT tangential band from 1593

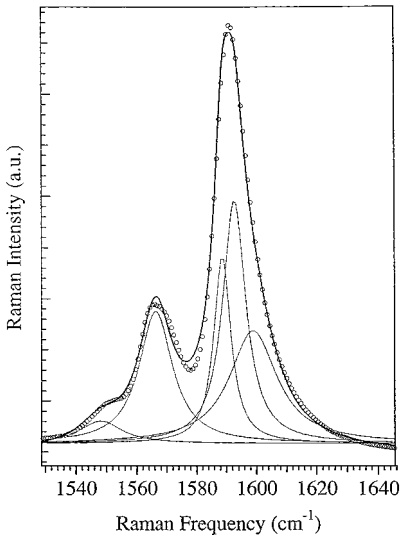

Figure 1. Broad tangential band for data collected from a pristine SWNT mat (open circles) with typical fit of five Lorentzians.

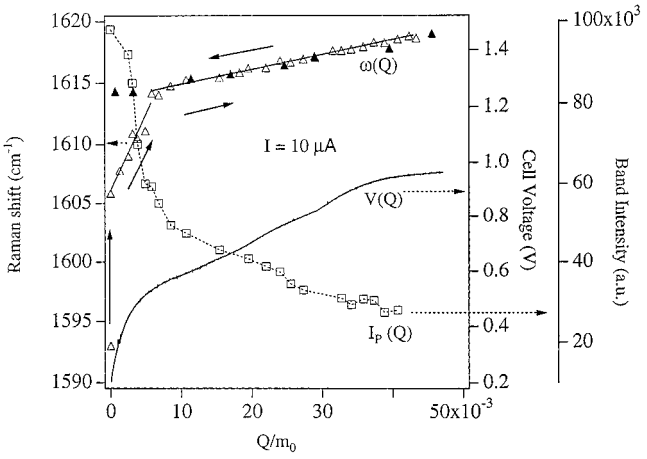

Figure 2. SWNT tangential band frequency ω, intensity I_p, and cell-potential V as a function of Q/m_0.

to 1604 cm^{-1} under *open circuit* (no external bias voltage) conditions. In the case of the graphite-H_2SO_4 system, no spontaneous (open circuit) shift of the 1582 cm^{-1} band was observed, and an external bias was necessary to induce intercalation and upshift the frequency of the ~1582 cm^{-1} Raman band. The fact that no remnant of the pristine SWNT band at 1593 cm^{-1} remained after only a few minutes (open circuit) contact with concentrated H_2SO_4 indicates that most of tubes in a typical bundle have spontaneously reacted to form a charge-transfer compound, presumably with a stoichiometry $C_p^+HSO_4^-\cdot xH_2SO_4$. This observation is perhaps not so surprising when it is recalled that (1) a charge-transfer GIC can also be prepared by boiling graphite in H_2SO_4[5] and (2) the interstitial volume in a nanotube bundle is very accessible. Unfortunately, since no external electrochemical current was passed to produce the spontaneous product, we cannot use coulometry and eq 1 to determine the charge transfer or stoichiometry of the spontaneously formed product.

It should be mentioned that the SWNT Raman band frequency we are discussing here is associated with the most intense (Lorentzian) contribution to a multiline, broad tangential band. In Figure 1, we show a typical fit of five Lorentzian components to the SWNT tangential band. As can be seen, one of these five components dominates the overall band area. Our line shape analysis showed that upon anodic oxidation, the frequencies of all these bands upshift together with charge transfer, and their *relative* intensities remain essentially constant, although their absolute intensity (integrated area) decreases strongly with intercalation and increased charge transfer. Therefore, for simplicity, we follow the behavior of the dominant Lorentzian component in the high-frequency tangential band, and from now on, when we refer to tangential band frequency, we are referring to this dominant component frequency.

In Figure 2, we also plot both the SWNT tangential band frequency ω and the cell potential V vs (Q/m_0), where (Q/m_0) is the electrochemical charge per unit initial SWNT electrode mass m_0. The data in Figure 2 were collected for a constant cell current of 10 μA using concentrated (18 M) H_2SO_4. The initial sudden jump $\Delta\omega$ of the Raman frequency noted at $Q = 0$ (i.e., $\Delta\omega = 12$ cm^{-1}) in Figure 2 is due to the spontaneous reaction discussed above. The open and solid triangles in Figure 2 refer to ω data collected on charging ($V_{Pt} - V_{SWNT} > 0$), and then on the subsequent discharging ($V_{SWNT} - V_{Pt} > 0$), of the cell. As can be seen in the figure, two nearly linear regimes for ω vs (Q/m_0) are observed. Once the cell potential exceeds ~0.5 V, a kink in the ω vs (Q/m_0) data is observed at $\omega \sim 1614$ cm^{-1} and subsequent ω vs (Q/m_0) data exhibit a more shallow slope. For this particular experiment, the current was reversed when the frequency reached ~1618 cm^{-1} and the ω vs (Q/m_0) data then retraced along the same curve with increasing reverse charge until the frequency reached 1614 cm^{-1} the second time. Continuing the reverse current was observed to have no further effect on the frequency, which was observed to remain constant at 1614 cm^{-1}. Above 0.5 V, the cell potential $V(Q)$ begins to exhibit a noticeably slower growth with increasing (Q/m_0). We identify the kink in the Raman data, and the concomitant decrease in the growth of the cell potential, with the onset of an "overoxidation" region for SWNT bundles, during which time C−O bonds form irreversibly. As in the case of graphite-H_2SO_4, this potential then corresponds to the upper limit for a simple charge-transfer reaction. "Overoxidation" is also consistent with the observation that frequencies below ~1614 cm^{-1} cannot be recovered by reversing the current; i.e., the SWNTs are irreversibly oxidized via the formation of C−O bonds. Furthermore, we should add that if a fresh SWNT electrode was studied, and the cell current was reversed before the tangential mode frequency reached 1614 cm^{-1}, the charge-transfer reaction could be reversed and the band frequency could be returned to 1604 cm^{-1}, i.e., the mode frequency returned to that reached by the spontaneous reaction of SWNTs in concentrated sulfuric acid.

We interpret the initial linear regime of ω vs (Q/m_0) induced by the electrochemical bias as follows. As a result of the spontaneous chemical reaction, the tube walls are decorated with HSO_4^- ions and neutral H_2SO_4 molecules and the cell potential climbs to 0.2 V. After the commencement of the galvanostatic charging, as the cell potential climbs from its initial value at 0.2 V to ~0.5 V, a mechanism similar, if not identical, to the "overcharging" mechanism observed in graphite-H_2SO_4 is identified with the increase in ω. In the "overcharging" regime, neutral H_2SO_4 molecules in the interstitial channels of the tube bundle are thereby converted to HSO_4^- (see reaction 3) and H_2 is lost from the electrode. Therefore, only a very small change in electrode mass should occur during overcharging, consistent with our mass uptake data to be discussed below. For charge neutrality of the SWNT bundle, the internal conversion of H_2SO_4 to HSO_4^- creates new holes in the SWNT π-band, and electrons are passed in the external circuit. However, the slope of the ω vs (Q/m_0) data in Figure 2 and eq 1 cannot be used to obtain a

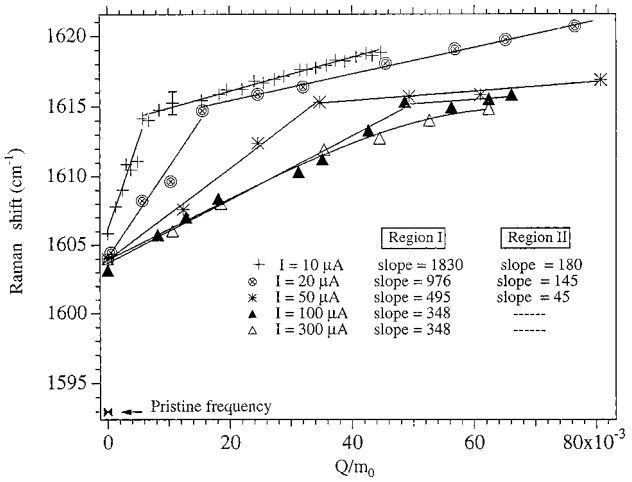

Figure 3. Raman shift ω vs Q/m_0 for the experimental runs with concentrated (18 M) H_2SO_4 acid at various constant currents. Typical error bar for the Raman shift (ω) is shown on the topmost curve.

"universal" value for this $d\omega/df$ for HSO_4^-·SWNT compounds (f = number of holes per C-atom). This is because a competing, spontaneous charge-transfer reaction must be accounted for. We discuss this below.

In Figure 3, we show the evolution of the tangential mode frequency, ω with (Q/m_0) for several choices of the cell current I_0, where $Q = I_0t$, and t is the time of the electrochemical reaction. As can be seen, the ω data for various values of I_0 in the range 10−300 μA all contain the characteristic kink at $\omega \sim$ 1614 cm^{-1}, which, as before, we identify with the onset of "overoxidation". Importantly, the slope of the linear regime in ω vs Q/m_0 between $Q = 0$ and the kink is seen to be a function of cell current (Figure 3). However, the slope saturates with increasing current to the value $d\omega/df = 348$ cm^{-1} per df = 1 hole per C-atom, as can be seen in the data collected for the higher cell currents of 100 and 300 μA. This behavior is identified with simultaneous contributions to charge transfer from a spontaneous side reaction and from the electrochemical overcharging reaction. Both reactions create holes (charge transfer) in the carbon π-band of the SWNT. At low currents, e.g., 10 μA, the side reaction contributes significantly to the overall charge-transfer rate, while at a factor of 10 higher current, (i.e., $I_0 > 100$ μA) the overall or total charge-transfer rate is then dominated by the electrochemical reaction and, in this case, eq 1 is then applicable.

To demonstrate that two types of simultaneous charge-transfer reactions are occurring in this system, we have analyzed the time evolution of the dominant tangential mode frequency ω with respect to the electrochemical cell current I_0. All these data were collected using 18 M H_2SO_4. Assuming that spontaneous *and* electrochemical charge-transfer reactions take place simultaneously, we write

$$(d\omega/dt) = (d\omega/dt)_e + (d\omega/dt)_s \quad (2)$$

where the subscripts e and s refer to the electrochemical and spontaneous reactions, respectively.

Now ($d\omega/dt$) can be expressed in terms of the rates R_e and R_s for charge transfer; that is,

$$(d\omega/dt) = R_e(d\omega/dQ)_e + R_s(d\omega/dQ)_s \quad (3)$$

where, $R_e = (dQ/dt)_e = I_0$, $R_s = (dQ/dt)_s$, and Q is the number of electrons removed from the carbon π-band via charge transfer to the dopant. We assume that $(d\omega/dQ)_e = (d\omega/dQ)_s \equiv (d\omega/dQ)$,

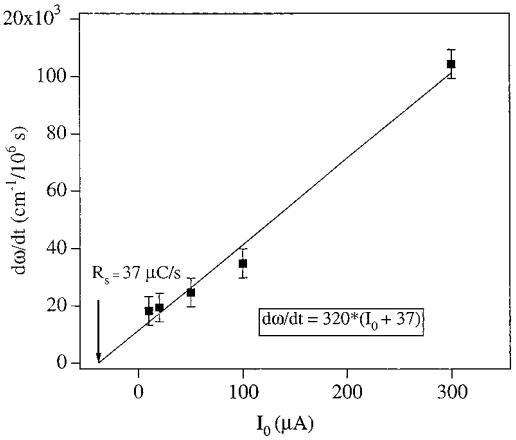

Figure 4. Intercalation rate ($d\omega/dt$) as a function of external current I_0 with the linear squares fit. The slope gives the intrinsic value of $d\omega/df$, and the x-axis intercept indicated by the downward arrow gives the spontaneous rate of charge transfer R_s.

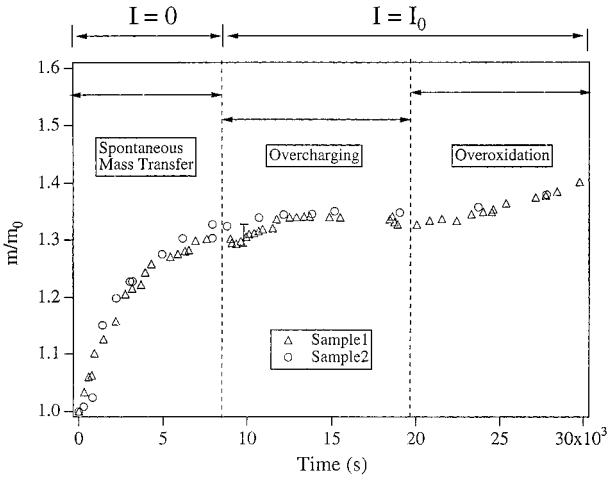

Figure 5. Time evolution of the SWNT electrode mass for two different samples.

since the upshift of ω should not depend on the reaction by which the charge transfer occurs. Hence, eq 3 can be written as,

$$(d\omega/dt) = (d\omega/dQ)[I_0 + R_s] \quad (4)$$

To assess the validity of the assumptions leading to eq 4, we plot in Figure 4 the experimental values of $d\omega/dt$ vs I_0 for fixed temperature T (∼24° C) and for concentrated (18 M) H_2SO_4. (R_s would, of course, depend on temperature and acid dilution.) In Figure 4, the squares represent the experimental data and the solid line is a linear least-squares fit to the data. As can be seen from the figure, the data are consistent with eq 4. From the fitting parameters we obtain $d\omega/df \sim 320$ cm^{-1}, and a value for the spontaneous charge-transfer rate is obtained, i.e., $R_s \sim$ 37 μC/s. Thus, we assign the value 320 cm^{-1} to the intrinsic value for the change in tangential mode frequency per hole, per C-atom created in the SWNT valence bands. For example, if this value were a universal result applicable to other acceptor−SWNT compounds, Raman scattering could be used to examine the charge transfer in a general $C_{10}^+X^-$ SWNT compound. In this case, a charge-transfer-induced upshift of 32 cm^{-1} in the tangential band should be observed, assuming the upshift is not particularly sensitive to the identity of the anion X^-.

Figure 5 shows the results of the time evolution of the SWNT electrode mass (m_0 = 50 mg) measured as described in the

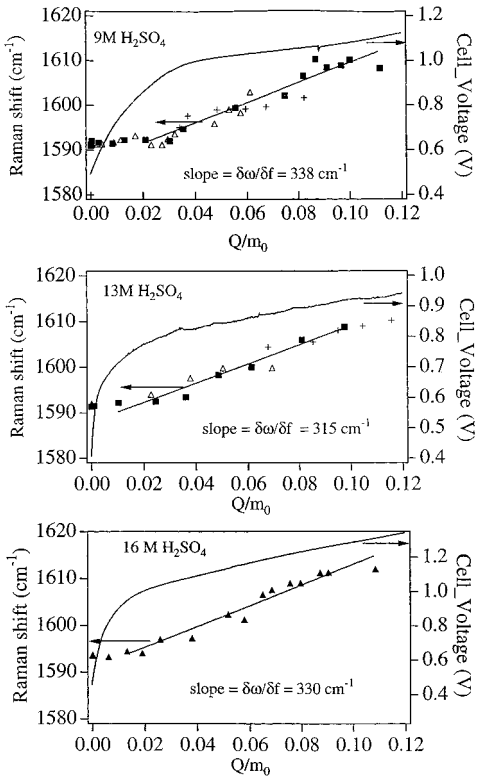

Figure 6. Effect of dilution on the observed chronopotentiometric profile and Raman shift of the tangential mode. Three dilutions are shown: 16, 13, and 9 M.

Experimental Section. It should be noted that data to the left of the first vertical dashed line are taken with the cell in the open circuit ($I_0 = 0$) condition, where a spontaneous reaction occurs, inserting HSO_4^- and H_2SO_4 into the tube bundles. During this time interval, the SWNT electrode mass is observed to increase and saturate at 130% of its original value (i.e., $1.3m_0$). This time interval is much longer than that observed for the tangential Raman band frequency to saturate. This behavior is consistent with the fact that the Raman scattering comes primarily from the SWNTs within the first several microns of the pressed mat sample and that additional time is required for the H_2SO_4 to diffuse and react in the interior of the sample (thickness of ~1 mm). After the saturation of the spontaneous mass uptake was observed, the cell current was initiated ($I = 1$ mA), and the cell potential and electrode mass were recorded as a function of time (Figure 5). In the region $V_{cell} < 0.5$ V, below the voltage threshold for "overoxidation", the mass is observed to be nearly constant, consistent with the proposed "overcharging" mechanism (i.e., internal conversion of H_2SO_4 to with an evolution of H_2).

We next discuss the effect on the electrochemical reaction of diluting the H_2SO_4 with H_2O. It is well-known that in the case of graphite in concentrated H_2SO_4, for each HSO_4^- anion, two acid molecules are cointercalated. Thus the use of concentrated acid that has a large concentration of undissociated acid molecules promotes this reaction and the use of dilute acid should diminish the reactivity. Similarly, it is expected that use of less reactive, dilute acid in the place of concentrated acid should prevent the spontaneous reaction of sulfuric acid with SWNTs.

The effect of H_2SO_4 dilution on the evolution of the tangential mode frequency ω in SWNTs with (Q/m_0) is shown in Figure 6 for three dilutions: 16, 13, and 9 M. At these concentrations, we observed at *current-independent* value for the charge-transfer-induced shift in the tangential SWNT dω/df. We interpret this observation as follows. Due to the acid dilution, the *spontaneous* charge-transfer reaction is apparently reduced and becomes relatively unimportant when compared to the electrochemical contribution at 30 μA (or higher currents). As can be seen in the figure, after initiation of the cell current, there is an initial short, "induction" period in which little change in the band frequency is observed. The mechanism behind the "induction" period is not understood, and further work is needed to sort this out. Another important difference to note between intercalation in concentrated and dilute H_2SO_4 is that, in dilute acid, we are able to fully deintercalate the sample under reverse bias, returning the Raman band frequency to the pristine value at 1593 cm^{-1}. This result is again consistent with a reduced forward spontaneous charge-transfer reaction, whereby the reverse electrochemical rate can be used to overwhelm the forward spontaneous rate. The observed values for dω/df obtained in dilute H_2SO_4 (315−340 cm^{-1}) are all in good agreement with the results obtained in concentrated (~18 M) acid, assuming simultaneous electrochemical and spontaneous charge-transfer reactions.

Conclusions

In conclusion, we have studied the anodic oxidation of SWNT bundles in sulfuric acid. Unlike previous similar electrochemical studies in H_2SO_4 GICs, an important spontaneous charge-transfer reaction competes with the electrochemical doping at lower currents. Similar to H_2SO_4 GICs, we were able to identify "overcharging" and irreversible "overoxidation" regimes in the electrochemical doping of the nanotube bundles. By analogy to graphite-H_2SO_4, we presume that the anion dopant is HSO_4^-. Our data indicate that both neutral H_2SO_4 and HSO_4^- reside in the interstitial channels between the tubes. The tangential Raman-active modes are found sensitive to charge transfer and we find a frequency upshift of 320 cm^{-1} per hole per C-atom introduced into the carbon π-band. This value may allow Raman scattering to provide a useful estimate for charge transfer in general acceptor-type SWNT compounds.

Acknowledgment. This work was supported, in part, by the U.S.DOE#DE-F22-90PC90029, NSF#OSR-9452895, and DMR-9809686 (MRSEC).

References and Notes

(1) Dresselhaus, M. S.; Dresselhaus, G. Intercalation Compounds of Graphite. *Adv. Phys.* **1981**, *30*, 139−326.
(2) Henning, G. R. *Prog. Inorg. Chem.* **1959**, *1*, 125.
(3) Rüdorff, W.; Hoffmann, U. *Z. Anorg. Allg. Chem.* **1938**, *238*, 1−50.
(4) Rüdorff, W. *Z. Phys. Chem. B* **1940**, *45*, 42.
(5) Schafhäutl, C.; *J. Prakt. Chem.* **1840**, *21*, 129.
(6) Blackman, L. C. F.; Mathews, J. F.; Ubbelohde, A. R. *Proc. R. Soc. A258* **1960**, 329.
(7) Bottomley, M. J.; Parry, G. S.; Ubbelohde, A. R.; Young, D. A. *J. Chem. Soc.* **1963**, 5674.
(8) Ubbelohde, A. R. *Carbon 2* **1964**, 23.
(9) Aronson, S.; Lemont, S.; Weiner, J. *Inorg. Chem.* **1971**, *10* (6), 1296.
(10) Aronson, S.; Frishberg, C. Frankl, G. *Carbon* **1971**, *9*, 715.
(11) Fujii, R.; Matsuo, K. *Tanso* **1973**, *73*, 44.
(12) Vogel, F. L. *J. Mater. Sci.* **1977**, 12, 982.
(13) Fischer, J. E. *Physica* **1980**, *99B*, 383.
(14) Metrot, A.; Fischer, J. E. *Synth. Met.* **1981**, *3*, 201.
(15) Fischer, J. E.; Metrot, A.; Flaunders, P. J.; Salaneck, W. R.; Brucker, C. F. *Phys. Rev. B* **1981** *23*, 5576.
(16) Salaneck, W. R.; Brucker, C. F.; Fischer, J. E.; Metrot, A. *Phys. Rev. B* **1981**, *24* (9), 5037.
(17) Berlouis, L. E. A.; Schiffrin, D. J. *J. Appl. Electrochem.* **1983**, *13*, 147.

(18) Bessenhard, J. O.; Wudy, E.; Möhwald, H.; Nickl, J.J.; Biberacher, W.; Foag, W. *Synth. Met.* **1983**, *7*, 185.
(19) Beck, F.; Krohn, H. *Synth. Met.* 1983, *7*, 193.
(20) Metrot, A.; Fuzellier, H. *Carbon* 1984, *22*, 131.
(21) Metrot, A.; Tihl, M. *Synth. Met.* 1985, *12*, 517.
(22) Beck, F.; Krohn, H.; Zimmer, E. *Electrochim. Acta* 1986, *31* (3), 371.
(23) Eklund, P. C.; Olk, C. H.; Holler, F. J.; Spolar, J. G.; Arakawa, E. T. *J. Mater. Res.* 1986, *1*(2), 361.
(24) Jiang, J.; Beck, F. *Carbon* 1992, *30*, 223.
(25) Avdeev, V. V.; Monyakina, L. A.; Nikol'Skaya, I. V.; Sorokina, N. E.; Semenenko, K. N. *Carbon* 1992, *30* (6), 819.
(26) Iwashita, N.; Shioyama, H.; Inagaki, M. *Synth. Met.* 1995, *73*, 33.
(27) Moissette, A.; Fuzellier, H.; Burneau, A.; Dubessy, J.; Lelaurain, M. *Carbon* 1995, *33* (2), 123.
(28) Dresselhaus, M. S.; Dresselhaus, G.; Eklund, P. C. *Science of Fullerenes and Carbon Nanotubes*; Academic Press: New York, 1996.
(29) Journet, C.; et al. *Nature* **1997**, *388*, 756.
(30) Thess, A. *Science* 1996, *273*, 483−487.
(31) Rao, A. M.; Eklund, P. C.; Bandow, S.; Thess, A.; Smalley, R. E. *Nature* 1997, *388*, 257−259.
(32) Lee, R. S.; Kim, H. J.; Fischer, J. E.; Thess, A.; Smalley, R. E. *Nature* 1997, *388*, 255−257.
(33) Grigorian, L.; Williams, K. A.; Fang, S.; Sumanasekera, G. U.; Loper, A. L.; Dickey, E. C.; Pennycook, S. J.; Eklund, P. C. *Phys. Rev. Lett.* 1998, *80*, 5560−5563.
(34) Bower, C.; Kleinhammes, A.; Wu, Y.; Zhou, O. *Chem. Phys. Lett.* 1998, *288*, 481−486.
(35) Beck, F.; Krohn, H.; Zimmer, E. *Electrochim. Acta* 1986, *31* (3), 371.
(36) Besenhard, J. O.; Mohwald, H.; Nickl, J. J. *Synth. Met.* **1981**, *3*, 187.
(37) Dresselhaus, M. S. *Raman Scattering in Carbon-based Materials*; Chapman and Hall: London, in press.
(38) Fiang, J.; Beck, F. *Carbon* 1992, *30* (2), 223.
(39) Metrot, A.; Fischer, J. E. *Synth. Met.* **1981**, *3*, 201.
(40) Minisci, F.; Citterio, A.; Giordano, C. *Acc. Chem. Res.* **1983**, *16*, 27.
(41) Metrot, A.; Fuzellier, H. *Carbon* **1984**, *22*, 131.
(42) Beck, F.; Krohn, H. *Synth. Met.* **1986**, *14*, 137.
(43) Eklund, P. C.; Arakawa, E. T.; Zaretsky, J. L.; Kamitakahara, W. A.; Mahan, G. D. *Synth. Met.* 1985, *12*, 97−102.